*Int. J. Electrochem. Sci.*, 13 **(2018)** 514 – 529, doi: 10.20964/2018.01.94

International Journal of
ELECTROCHEMICAL
SCIENCE
www.electrochemsci.org

# Linseed Oil Based Amide as Corrosion Inhibitor for Mild Steel in Hydrochloric Acid

*Z.N. Yang, Y.W. Liu, Y. Chen*[*]

College of Chemistry & Chemical Engineering, Binzhou University, Binzhou, Shandong 256600, China
[*]E-mail: chen123yu123@163.com

*Received:* 6 August 2017 / *Accepted:* 27 September 2017 / *Online Published:* 1 December 2017

A new inhibitor named linseed oil amide (LOA) has been synthesized. The molecule structure of LOA was characterized with Fourier transform infrared spectroscopy and its inhibition behavior for mild steel in hydrochloric acid was measured by weight loss, potentiodynamic polarization, electrochemical impedance spectroscopy (EIS) and scanning electron microscopy. Weight loss measurements reveal that the corrosion rate was dependent on the concentration of the inhibitor, which decreases with increasing the LOA inhibitor concentration. Both of the anodic and cathodic are inhibited according to the potentiodynamic polarization results, while the cathodic effect is more pronounced, which indicates that the LOA inhibitor acts as a mixed-type with predominant control of cathodic reaction. The adsorption of LOA onto mild steel in hydrochloric acid follows Langmuir adsorption isotherm. Activation parameters are calculated and discussed, which imply the endothermic nature of the mild steel dissolution process and the adsorption of LOA inhibitor acts mainly as chemisorptions. The inhibition efficiency is still over 90% after immersion of 96 h, suggesting the long-term effective property of LOA inhibitor.

**Keywords:** inhibition; mild steel; EIS; hydrochloric acid

## 1. INTRODUCTION

Iron and its alloys have been widely used for industrial applications, while exposed to highly corrosive media in several industrial processes, such as acid pickling, industrial cleaning and oil-well acidification whose aggressive property may cause critical damage [1,2]. There are several ways to control the corrosion process and among them the utilization of inhibitors is usually the most practical and effective one to prevent the corrosion. Studies have showed that organic compounds containing both sulphur and nitrogen atom with high electron density and those with multiple bonds can adsorb onto the metal surface, which are considered to be excellent inhibitors [3-5]. However, as a result of increasing awareness of toxic risks to environment and humans, attentions have been paid to searching

for “green” and “non-toxic” corrosion inhibitors [6-8]. Therefore, the natural products, such as plant extracts [9-12], vegetable oils and its derivatives [13-15] have attracted much more interest for their environmental friendless. Linseed oil can be easily found in the Northwest district of China as one of the main economic crops which has been applied to perform different kinds of polymeric resins [16] for its unique structure compared to other kinds of vegetable oil. The imidazoline inhibitor based on linseed oil has been reported in our previous work [17] to inhibit the mild steel corrosion in acidic medium which shows a maximum inhibition efficiency of 85%, while the preparation of this inhibitor is so complicated and the product yield is very low. In addition, the long-term efficiency has not been investigated.

In the present work, an environment friendly inhibitor of linseed oil amide (LOA) was synthesized by amidation reaction with a high yield. The inhibition behavior of LOA for mild steel in hydrochloric acid was systematically investigated by weight loss, potentiodynamic polarization, electrochemical impedance spectroscopy (EIS) and the corroded steel surface was characterized by scanning electron microscopy (SEM).

## 2. EXPERIMENTAL

### *2.1. Materials*

The corrosive solution 1.0 M hydrochloric acid was prepared from analytical reagent grade HCl and double distilled water. The linseed oil amide was synthesized by amidation reaction of linseed oil (Sigma-Aldrich Co., USA) and diethylenetriamine (Sinopharm Chemical Reagent Co. Ltd) in xylene media with $N_2$ [17]. Briefly, 12.4 g (0.12 mol) diethylenetriamine was dissolved in 40 ml xylene in a four-neck round bottom flask fitted with electrical stirrer, dropping funnel, thermometer and a condenser. Then, 28.0 g (containing 0.1 mol linolenic oil structure) was added in drops into the flask for half an hour at about 110 °C with electrical stirring rate of 600 rpm. Lately, the mixture was subsequently electrically stirred at about 120 °C for another two hours to convert all oil into amide. Finally, the solvent was removed by rotary evaporation and the product linseed oil amide was further purified in a chromatographic column of silica-gel using the mixture of trichlromethane and absolute methanol (V:V=6:1) with a yield of 95.3%. The purified linseed oil amide (designed as LOA) was characterized by FTIR (Nexus670, NICOLET) in the wave-number range from 400 to 4000 $cm^{-1}$.

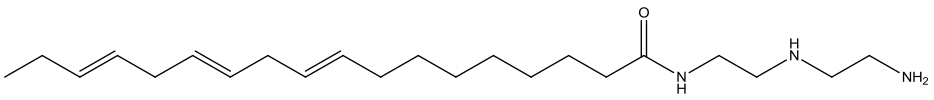


**Figure 1.** Structure of linseed oil amide (LOA)

### *2.2. Weight loss measurement*

The weight loss measurements were carried out in 1.0 M HCl solution at 40°C for 4 h using an analytical balance. Square specimens with dimensions 50 mm × 25 mm × 5 mm were used. The

specimens were accurately weighted and then immersed into 1.0 M HCl solution without or with different concentration of LOA which was dissolved in 2 ml isopropanol first. After 4 h of immersion period, the specimens were taken out, scrubbed with bristle brush, rinsed with double distilled water and acetone, dried at room temperature and then weighted. Triplicate experiments were performed in each case and the average value of the weight loss was used to calculate the corrosion rate in millimeters per year (mm $y^{-1}$) and inhibition efficiency ($\eta$) in percent (%) with the following equation [18,19]:

$$CR = \frac{K \times W}{A \times t \times \rho} \quad (1)$$

$$\eta(\%) = (1 - W_{inhi}/W_{free}) \times 100\% \quad (2)$$

Where K is a constant of $8.76*10^4$, W is the mass loss in gram, A is the surface area in $cm^2$, t is the immersion time in hours and ρ is the density in g $cm^{-3}$ with the value of $7.86*10^3$, $W_{inhi}$ and $W_{free}$ are the weight loss in presence and absence of LOA inhibitor, respectively.

### *2.3. Electrochemical experiment*

Electrochemical experiments were carried out in a traditional three-compartment cell. A saturated calomel electrode (SCE) connected through a salt bridge was used as reference, and a large area platinum foil as counter electrode. The working electrode (Q235 mild steel) which had a geometrical working area of 0.50 $cm^2$ was polished to mirror using 2.5 μm diamond paste, washed with double-distilled water, rinsed with acetone, dried at room temperature and stored in desiccators prior to each measurement. All potentials not otherwise specified in this paper were referred to SCE.

Prior to each electrochemical measurement, the working electrode was immersed into the corrosive solution until the open-circuit potential reached constant, indicating a steady state of the working electrode surface. Potentiodynamic polarization studies were performed using electrochemical workstation (CHI660A, China) at a scan rate of 1 mV/s. Electrochemical impedance spectroscopy (EIS) measurements were carried out in the frequency range from 100 KHz to 10 mHz with the voltage amplitude of 5 mV at $E_{corr}$ using an impedance measurement unit (PARSTAT 2273, Advanced Electrochemical System). Each test was repeated three times or more in parallel with the relative deviation less than 5%.

### *2.4. Surface analysis*

The surface morphological characteristics of the inhibited and uninhibited mild steel samples were observed using scanning electron microscope (Hitachi S-4800).

## 3. RESULTS AND DISCUSSION

### *3.1. Structure study*

Fig.2 shows the infrared spectrogram of linseed oil and the obtained LOA, respectively. The FTIR spectrum peaks at 2960 $cm^{-1}$ and 2842 $cm^{-1}$ are associated with asymmetric stretching and symmetric stretching vibration of $–CH_3$ and $–CH_2$, respectively. Characteristic peak at 1735 $cm^{-1}$ may be related to the O=C-O structure in linseed oil molecule. Another two new absorption peaks compared to that of the linseed oil which appeared at 1652 $cm^{-1}$ and 1546 $cm^{-1}$, is a characteristic of amide bond of -(C=O)-NH- in this synthesized LOA molecule.

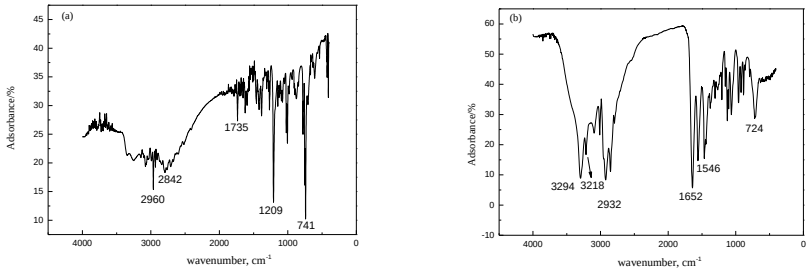


**Figure 2.** FTIR of the (a) linseed oil; (b) obtained LOA.

Meanwhile, the band near 3294 $cm^{-1}$ and 3218 $cm^{-1}$ may be correlated to N-H band stretching vibrations. This result was identical with those found in reference [20]. Therefore, the FTIR result confirms that the synthesized product is LOA.

### *3.2. Weight loss measurements*

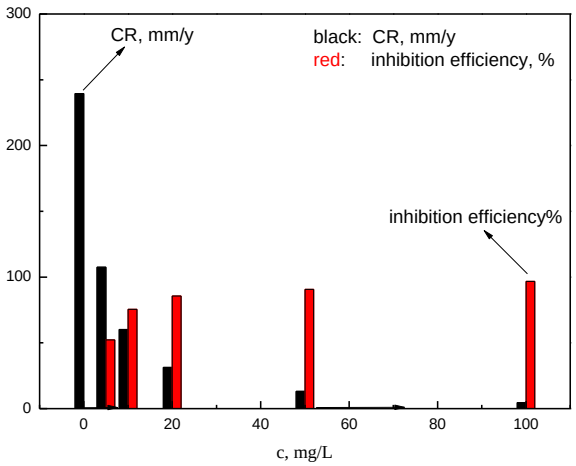


**Figure 3.** Weight loss measurements for mild steel in 1.0 M HCl solutions without and with different concentrations of LOA inhibitor at 40 °C for 4 h.

The weight loss results in the absence and presence of different concentrations of LOA inhibitor in 1.0 M HCl at 40 °C for 4 h are provided in Fig.3. It is very clear that the corrosion rate is smaller in the inhibited solutions compared to the uninhibited solution, suggesting the formation of a protective film by LOA inhibitor at the metal surface which suppressed the mild steel dissolution in 1.0 M HCl solution [21]. Meanwhile, the corrosion rate decreases with the increase of inhibitor concentration, consequently, the inhibition efficiency increases with the addition of higher concentrations LOA inhibitor. The inhibition efficiency is 55.1% although the concentration of LOA inhibitor is 5 mg/L, indicating that a protective film has been formed on the mild steel surface and the inhibitor LOA effectively retards the dissolution of mild steel in the aggressive environment [22]. The maximum inhibition efficiency of 98.1% was achieved at 100 mg/L, which is much higher than that of the inhibitor prepared from red pepper seed oil [23].

### *3.3. Potentiodynamic polarization curves*

Fig.4 shows the potentiodynamic polarization curves in the absence and presence of different concentrations of LOA inhibitor for mild steel in 1.0 M HCl solution at 40 °C. It can be seen that both the cathodic and anodic current densities decreased with the addition of LOA inhibitor, suggesting that the LOA inhibitor retard both the cathodic and anodic branch, corresponding to the hydrogen evolution reaction and steel dissolution process, respectively. Apparently, the current density of cathodic branch decay more sharply compared to the anodic branch. Noticeably, the addition of LOA inhibitor resulted in shifting the corrosion potential to more negative values, which maximum corrosion potential was shifted -81 mV compared to that of the blank.

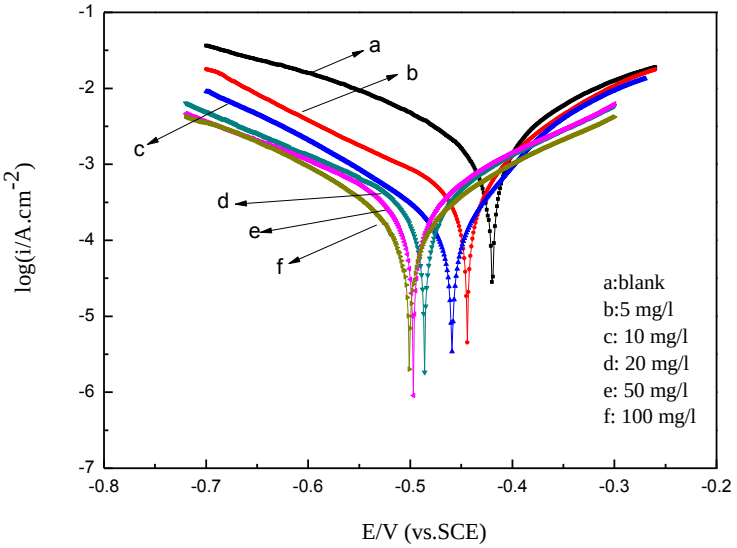


**Figure 4.** Polarization curves of Q235 mild steel in 1.0 M HCl solutions with different concentration of LOA inhibitor at 40 °C for 1 h.

Both of these phenomenon indicated that the LOA inhibitor acts as a mixed-type with predominant control of cathodic reaction [24,25]. Meanwhile, it is also clear that the shape of both the

anodic and cathodic Tafel curves in the absence of LOA inhibitor are similar to that in the presence of different concentration of LOA inhibitor, meaning that the addition of LOA inhibitor did not change the corrosion mechanism of mild steel in hydrochloric acid [26-28]. In another word, the corrosion inhibition of LOA inhibitor is caused by blocking the active sites on the mild steel surface without modifying the corrosion mechanism in this aggressive media. Moreover, to gain the kinetics behavior of the dissolution process, parameters such as corrosion potential ($E_{corr}$), corrosion current density ($j_{corr}$), anodic Tafel slope ($\beta_a$) and cathodic Tafel slope ($\beta_c$) obtained by extrapolation of Tafel lines are given in Table 1.

The corrosion inhibition efficiency ($\eta$) and the surface coverage ($\theta$) are calculated using $j_{corr}$ values with the following equations (3) and (4) [29], whose results are also listed in Table 1.

$$\eta = (1 - I_{inhi} / I_{free}) \times 100\% \quad (3)$$

$$\theta = 1 - I_{inhi} / I_{free} \quad (4)$$

Where $j_{inhi}$ and $j_{free}$ are the corrosion current density with and without LOA inhibitor respectively.

From Table 1, it is obvious that $E_{corr}$ shifted to the negative direction and the corrosion current density of mild steel in the presence of inhibitor LOA decreased significantly as compared in the absence of inhibitor, mainly attributed to the fact that the LOA inhibitor adsorb on the mild steel surface, forming a protective passive film and retarding the corrosion reaction. With the increase of the LOA inhibitor concentration, $j_{corr}$ simultaneously decreased and reached a minimum value at the LOA concentration of 100 mg/l, consequenctly the maximum value of inhibition efficiency of 91.2%, likely due to a greater number of inhibitor molecules covering the mild steel surface at this concentration [30]. This result also agrees well with the weight loss measurement as the corrosion rate is directly proportional to the corrosion current density ($j_{corr}$).

**Table 1**. Electrochemical polarization parameters for Q235 mild steel in 1.0 M HCl solution containing different concentration of LOA inhibitor at 40 °C for 1 h.

| c, mg/L | $E_{corr.}$ (mV vs. SCE) | $j_{corr.}$ ($mA.cm^{-2}$) | $B_a$ ($mV.dec^{-1}$) | $-B_c$ ($mV.dec^{-1}$) | η% | θ |
|---|---|---|---|---|---|---|
| 0 | -420 | 1.121 | 118 | 198 | | |
| 5 | -444 | 0.534 | 116 | 174 | 52.4 | 0.524 |
| 10 | -459 | 0.392 | 124 | 169 | 65.1 | 0.651 |
| 20 | -486 | 0.183 | 112 | 183 | 83.7 | 0.837 |
| 50 | -497 | 0.128 | 116 | 190 | 88.6 | 0.886 |
| 100 | -501 | 0.099 | 119 | 176 | 91.2 | 0.912 |

*3.4. EIS measurements*

EIS measurements (Fig.5) of the mild steel electrode at its open circuit potential were recorded after 1 h of immersion in the inhibited as well as uninhibited 1.0 M HCl solution. It can be seen that the addition of LOA inhibitor into acid solution had significant influence on the impedance response. With increasing the LOA concentration, the size of semicircle increases as well, indicating that the

inhibitor adlayers had been formed on the mild steel surface and this protective film could protect iron from corrosion in the hydrochloric acid solution. The EIS plots also show that, there is only one large capacitive loop in low concentration range (5 - 20 mg/l), while one more loop in higher LOA concentration (50 mg/l, 100 mg/l), ascribed to the double layer capacitance and the protective action of inhibitor adlayer formed on the metal surface, respectively [31]. Meanwhile, the capacitive loop show depressed semicircle, which is attributed to the dispersion effect due to the roughness and non-homogeneity of working electrode surface [32]. Thus, the constant phase element (CPE) is used instead of capacity, which is described as follows [33-35]:

$$Z_{CPE} = \frac{1}{Y_0 (j\omega)^n} \qquad (5)$$

Where $Y_0$ is CPE constant, $\omega$ is the frequency, and $n$ is the phase shift which can be explained as a degree of surface inhomogeneity.

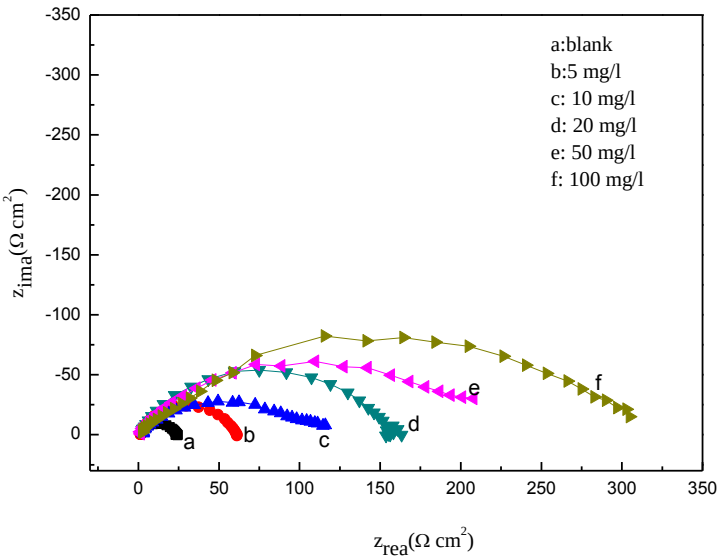


**Figure 5.** Nyquist plots of Q235 mild steel in 1.0 M HCl solutions with different concentration of LOA inhibitor at 40 °C for 1 h.

Two different equivalent electrical circuits (EEC) model shown in Fig.6 are employed to simulate the EIS data using non-linear-least-square fit analysis (NLLS) software and the analyzed impedance parameters are listed in Table 2. The elements of the circuit can be named as: $R_s$ is the solution resistance, $CPE_{dl}$ represents the double layer capacitance, $R_{ct}$ is the charge transfer resistance. Two new elements of $CPE_f$ and $R_f$ as shown in Fig.6(b), corresponding to the film capacitance and resistance respectively, were added into the equivalent circuit to explain the adsorption of LOA inhibitor onto the metal surface [36].

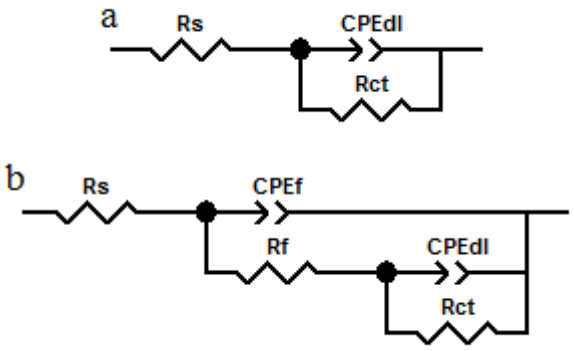


**Figure 6.** EEC used for simulating the impedance spectra: (a) with one time constant; (b) with two time constants.

The total polarization resistance ($R_p$) for Q235 mild steel in 1.0 M HCl solutions with different concentration of LOA inhibitor must be equal to the sum of $R_f$ and $R_{ct}$, which has been reported by other researchers [37,38]. Therefore, the inhibition efficiency $\eta$ was calculated by the following equation, and the results are also listed in Table 2:

$$\eta = (1 - R_p^{free} / R_p^{inhi}) \times 100\% \qquad (6)$$

where $R_p^{free}$ and $R_p^{inhi}$ are the total polarization resistances without and with LOA inhibitor, respectively.

**Table 2**. EIS parameters for Q235 mild steel in 1.0 M HCl solutions with different concentration of LOA inhibitor at 40 °C for 1 h.

| Concentration mg/L | $R_s$ $\Omega.cm^2$ | $CPE_f$ $\mu F.cm^{-2}$ | $R_f$ $\Omega.cm^2$ | $CPE_{dl}$ $\mu F.cm^{-2}$ | $R_{ct}$ $\Omega.cm^2$ | η% |
|---|---|---|---|---|---|---|
| 0 | 1.26 | | | 225 | 17.6 | |
| 5 | 1.67 | | | 156 | 70.9 | 75.2 |
| 10 | 1.61 | | | 110 | 91.9 | 80.8 |
| 20 | 1.84 | | | 56.8 | 166 | 89.4 |
| 50 | 1.62 | 202 | 24.5 | 43.2 | 204 | 91.4 |
| 100 | 1.72 | 138 | 33.2 | 28.6 | 260 | 93.2 |

The fitting results of mild steel corrosion in 1.0 M HCl solutions with different concentration of LOA inhibitor were given in Table 2. It is apparent that, in the concentration range of LOA inhibitor from 0-100 mg/l, the value of double layer capacitance $CPE_{dl}$ decreases with increasing the LOA inhibitor concentration, mainly related to the replacement of water molecules on the steel surface by LOA inhibitor molecules which have small dielectric constant compared to the water molecules. The relationship between dielectric constant and $CPE_{dl}$ is expressed by equation [39]:

$$CPE_{dl} = \frac{\varepsilon\varepsilon_0 A}{d} \qquad (7)$$

Where $\varepsilon$ is the dielectric constant, $\varepsilon_0$ is the vacuum permittivity, $A$ is the effective area of the electrode and $d$ is the thickness.

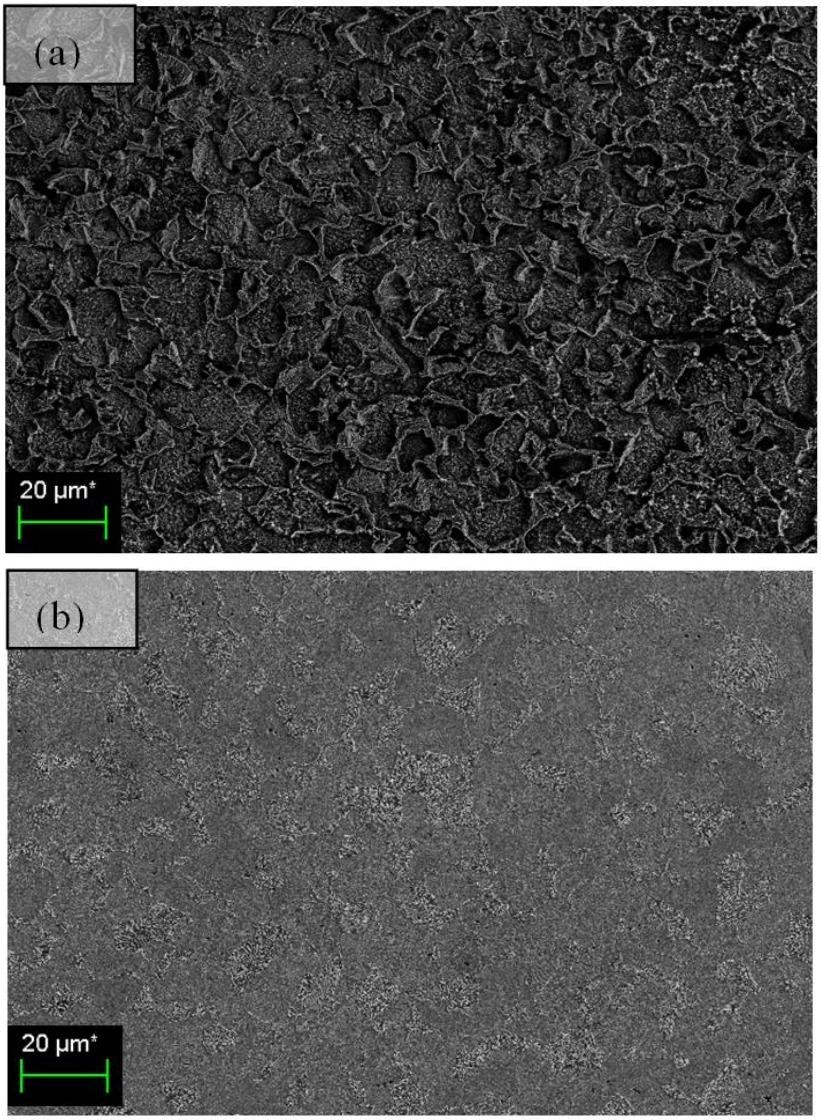


**Figure 7.** SEM images of Q235 mild steel samples after immersion in 1.0 M HCl for 1 h without (a) and with (b) 100 mg/L LOA inhibitor.

Meanwhile, the charge transfer resistance $R_{ct}$ of the corrosion of mild steel increases as the LOA concentration increases, whose value changes from 17.6 $\Omega.cm^2$ to 260 $\Omega.cm^2$ (Table 2). Moreover, an increase of the inhibition efficiency from 75.2% to 93.2% of LOA was also observed with increasing the LOA concentration to 100 mg/L. The result is in perfect agreement with that obtained by polarization technique.

The morphologies of mild steel surface were analyzed after immersion in acid solution for 1 h without and with 100 mg/L LOA inhibitor, are shown in Fig.7. The micrographs clearly reveal that the mild steel surface is highly rough and considerably destroyed in the absence of LOA inhibitor, while adding 100 mg/L LOA inhibitor into the 1.0 M HCl solution, the mild steel surface mostly seems

smooth, indicating that the LOA inhibitor can provide a stable barrier on the steel surface. Therefore, it can be concluded that the LOA is a good inhibitor for Q235 mild steel in acid solution.

### *3.5. Adsorption isotherm*

It is known that the adsorption process is a substitution reaction that adsorbed water molecules are replaced by inhibitor molecules which occurs between the metal/solution interface [40]. To get a better understanding of the LOA adsorption mechanism on mild steel surface, some adsorption isotherms (Temkin, Langmuir, Flory-Huggins, Frumkin,…) were assessed and Langmuir adsorption isotherm was found to be the most suitable isotherm with the experimental data. The linear relationship between $c/\theta$ and $c$ obtained from gravimetric measurements is shown in Fig.8, which conforms to the Langmuir Adsorption isotherm with the following equation [41]:

$$c/\theta = 1/K_{ads} + c \qquad (8)$$

Where $c$ is the LOA concentration; $\theta$ is the surface coverage obtained from weight loss measurements, and $K_{ads}$ is the equilibrium constant of the LOA inhibitor adsorption process, which can be calculated from the intercepts of Fig.8.

$K_{ads}$ is related to the adsorption standard free energy $\Delta G^0_{ads}$, according to the equation [42]:

$$K_{ads} = \frac{1}{55.5} \times \exp(-\Delta G^0_{ads}/RT) \qquad (9)$$

Where 55.5 is the molar concentration of water in solution, $R$ is the gas constant and $T$ is the absolute temperature.

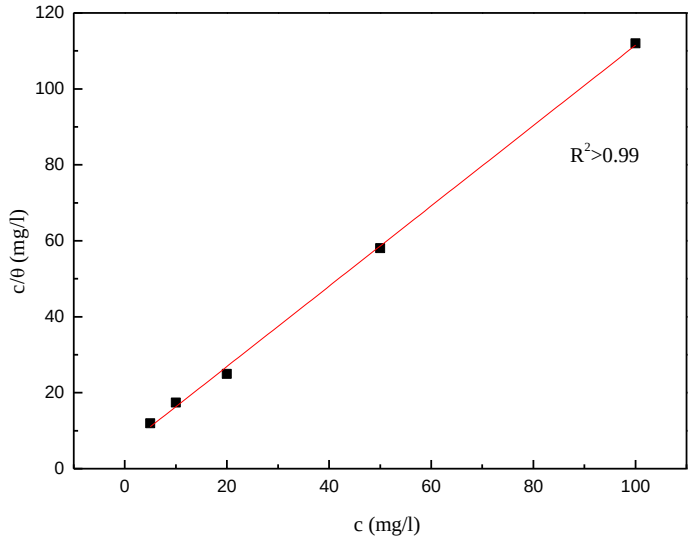


**Figure 8.** Langmuir adsorption isotherm for LOA inhibitor onto Q235 mild steel in 1.0 M HCl solution.

It is generally believed that absolute value of $\Delta G^0_{ads}$ higher than -20 KJ/mol is consistent with physical adsorption mechanism, while smaller than -40 KJ/mol corresponds to the chemical adsorption

mechanism [43]. $\Delta G_{ads}^{0}$ of LOA adsorption onto mild steel is found to be -40.5 kJ/mol in this work. This large negative value suggests that LOA inhibitor spontaneously adsorbed on the mild steel, and the adsorption reaction is mainly chemisorption, in which the covalent bond is formed by the charge sharing or transfer from organic molecule to the metal *d* orbit [44]. Actually, the electron-donating groups of N, O, and π electrons in the LOA molecules, through which the LOA formed a coordinate type of bond with the vacant 3*d* orbital of the mild steel surface, resulted in a protective chemisorbed film. Besides, the long chain ($CH_2$-$CH_2$) group provides an effective barrier from the aggressive medium.

### *3.6. Effect of temperature*

To evaluate the thermodynamic and activation parameters of LOA inhibitor adsorption on mild steel surface, weight loss experiments were also conducted in the temperature range from 20 °C to 60 °C which was performed with LOA inhibitor concentration of 100 mg/L for immersion time of 4 h. The dependence of corrosion rate and inhibition efficiency on testing temperature is shown in Table 3. The effect of temperature on the inhibition behavior is complicated which influences the adsorption equilibrium and kinetics as well [45,46]. It is clear from Table 3 that the corrosion rate increases with increasing temperature. Due to more desorption of LOA inhibitor molecules at higher temperature, greater surface active sites comes in contact with aggressive environment, thus, causing increased corrosion rate with increasing the temperature. In addition, it is noticeable that the inhibition efficiency of LOA inhibitor for Q235 mild steel in 1.0 M HCl solutions gets higher when the testing temperature increases from 30°C to 60°C. This phenomenon has also been reported by Ammar [47] and explained by the lower desorption rate than adsorption at higher temperature [48,49].The opposite processes of adsorption and desorption of inhibitor molecules are in equilibrium at a certain temperature. With increasing the temperature, the equilibrium is shifted leading to a higher adsorption rate than desorption until a new equilibrium is established with a higher equilibrium constant, resulting in the higher inhibition efficiency at higher temperature. Furthermore, according to literatures [50,51], the increase of inhibition efficiency with temperature suggests chemisorption of inhibitor molecular onto mild steel surface. Consequently, it is rational to infer that the LOA inhibitor was chemisorption on the mild steel surface in our experimental conditions. The proposed adsorption process is given in Figure 9.

**Table 3**. Values of corrosion rate and inhibition efficiency for Q235 mild steel in 1.0 M HCl solutions with 100 mg/L LOA inhibitor at different temperatures.

| Temperature °C | Corrosion rate mm/y | η% |
|---|---|---|
| 30 | 3.54 | 95.0 |
| 40 | 4.59 | 96.8 |
| 50 | 6.14 | 98.2 |
| 60 | 8.62 | 99.2 |

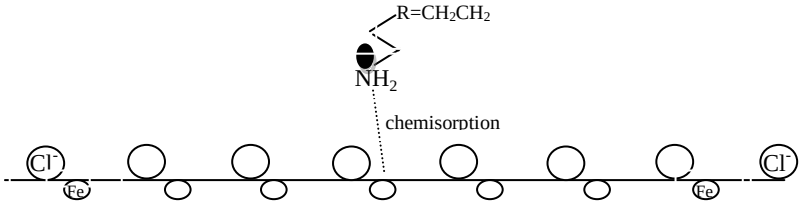


**Figure 9.** Schematic illustration of LOA inhibitor adsorption mechanism on Q235 mild steel in 1.0 M HCl solutionr.

The activation parameters, such as apparent activation energy ($E_a$), enthalpy ($\Delta H_a^0$) and entropy ($\Delta S_a^0$) for mild steel dissolved in 1.0 M HCl solution in absence and presence of 100 mg/L LOA inhibitor can be calculated with Arrhenius equation and transition state equation [52,53]:

$$\log(CR) = \frac{-E_a}{2.303RT} + \log\lambda \qquad (10)$$

$$CR = RT / Nh \exp(-\Delta H_a^0 / RT) \exp(\Delta S_a^0 / R) \qquad (11)$$

Where CR is the corrosion rate at different testing temperature, $E_a$ is the apparent activation energy, R is the universal gas constant of 8.314, T is the absolute temperature and λ is the Arrhenius preexponential factor. N is Avogadro's number and h is Plank's constant.

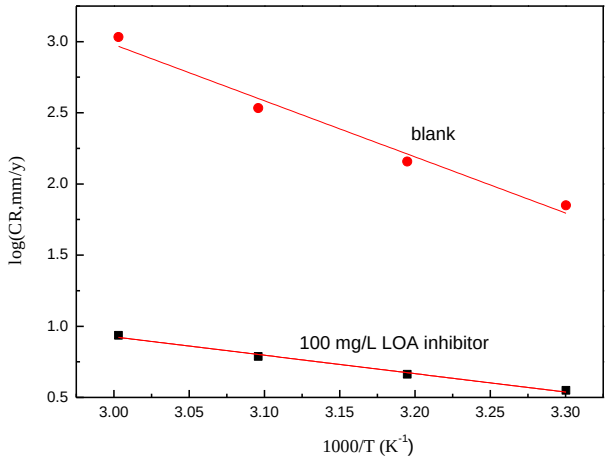


**Figure 10.** Arrhenius plots of log (CR) vs 1000/T for Q235 mild steel in 1.0 M HCl solution in absence and presence of 100 mg/L LOA inhibitor.

**Table 4**. Values of activation parameters $E_a$, $\Delta H_a^0$, $\Delta S_a^0$ for Q235 mild steel in 1.0 M HCl solutions without and with 100 mg/L LOA inhibitor.

| Inhibitor | $E_a$ KJ mol$^{-1}$ | $\Delta H_a^0$ KJ mol$^{-1}$ | $\Delta S_a^0$ J mol$^{-1}$ K$^{-1}$ |
|---|---|---|---|
| blank | 75.5 | 72.8 | -5.23 |
| 100 mg/L | 24.8 | 22.1 | -30.4 |

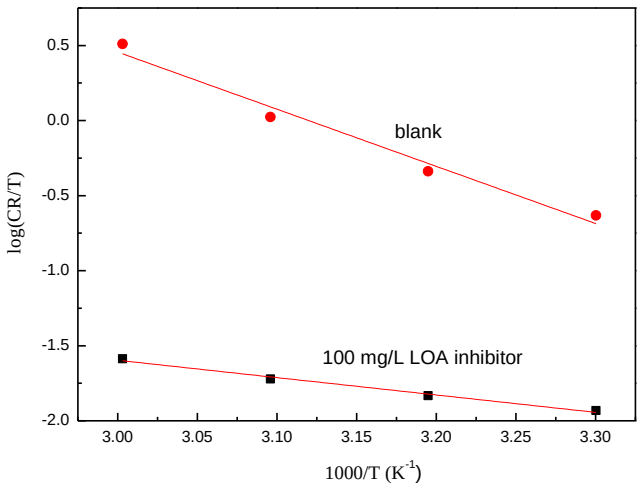


**Figure 11.** Arrhenius plots of log (CR/T) vs 1000/T for Q235 mild steel in 1.0 M HCl solution in absence and presence of 100 mg/L LOA inhibitor.

Fig.10 shows the Arrhenius plots of log (CR) vs 1000/T for Q235 mild steel in 1.0 M HCl solution in absence and presence of 100 mg/L LOA inhibitor. The slope ($\frac{-E_a}{2.303R}$) of the straight line can be used to calculate the activation energy $E_a$. The linear relationship of log (CR/T) vs 1000/T was also found, as shown in Fig.11, which can be applied to calculate enthalpy ($\Delta H_a^0$) and entropy ($\Delta S_a^0$) from the slope and intercept, respectively. Values of these activation parameters for Q235 mild steel in 1.0 M HCl solutions without and with 100 mg/L LOA inhibitor are all listed in Table 4.It can be seen that $E_a$ decreases with addition of LOA inhibitor compared to the blank, indicating the chemisroption mechanism of LOA inhibitor on mild steel surface [54,55], which is in good agreement with the adsorption standard free energy analysis. In addition, the positive value of $\Delta H_a^0$ suggests the endothermic nature of the mild steel dissolution process and the enthalpy for Q235 mild steel in 1.0 M HCl solution in presence of 100 mg/L LOA inhibitor (22.1 KJ $mol^{-1}$) is lower than that of in the absence of LOA inhibitor (72.8 KJ $mol^{-1}$), suggesting easier adsorption of LOA inhibitor on mild steel surface which results into high inhibition efficiency. Furthermore, the value of $\Delta S_a^0$ is negative which implies the loss of translation freedom by the adsorption of LOA molecular on mild steel surface [56].

### *3.7. Effect of immersion time*

The effect of immersion time on the inhibition efficiency for 100 mg/L LOA inhibitor onto Q235 mild steel in 1.0 M HCl solution is depicted in Fig.12. It is apparent that after 96 h immersion, the inhibitor efficiency is still over 90%, which indicates that LOA is a long-term effective inhibitor for mild steel in 1.0 M HCl solution. It is noticeable that inhibition efficiency increases with immersion time in the initial 8 h, which may be due to the slow adsorption and rearrangement of the LOA molecular on the mild steel surface. While after immersion of 8 h, the inhibition efficiency

decreases with immersion time which probably lies in desorption of available inhibitor molecules in the solution [46].

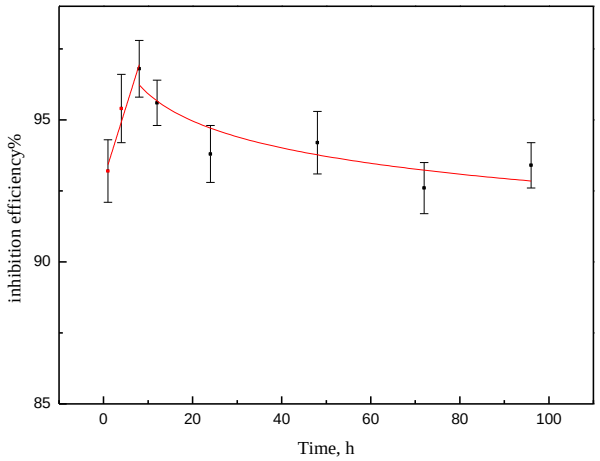


**Figure 12.** Effect of immersion time on the inhibition efficiency for 100 mg/L LOA inhibitor onto Q235 mild steel in 1.0 M HCl solution.

## 4. CONCLUSIONS

Linseed oil amide has been synthesized and characterized with FTIR. The inhibition behavior has been investigated using weight loss and electrochemical techniques. Results show that LOA is an effective inhibitor for mild steel in 1.0 M HCl solutions and acts as a mixed-type inhibitor with predominant control of cathodic reaction. Meanwhile, the inhibition efficiency increases with increasing concentration and reaches a maximum value at 100 mg/L. Weight loss measurements are in good agreement with the results of potentiodynamic polarization and electrochemical impedance spectroscopy. The adsorption of LOA on mild steel in 1.0 M HCl solutions is chemisorption, and follows Langmuir adsorption isotherm. The activation parameters suggest the endothermic nature of the mild steel dissolution process. Moreover, the inhibition efficiency is still over 90% after immersion of 96 h, revealing the long-term effective property of LOA inhibitor.

ACKNOWLEDGEMENTS
The authors wish to acknowledge the financial supports of the National Natural Science Foundation of China (Project 21403194), the Doctoral Research Foundation of Binzhou University (2017Y01), the Scientific Research Award Foundation for Shandong Provincial (ZR2014EMQ007) and the Major Project of Binzhou University (2016ZDW03).

## References

1. E.E. Oguzie, *Mater. Lett.* 59 (2005) 1076.
2. Z.Y. Hu, Y.B. Meng, X.M. Ma, H.L. Zhu, J. Li, C. Li and D.L. Cao, *Corros. Sci.* 112 (2016) 563.
3. P. Mourya, S. Banerjee and M. Singh, *Corros. Sci.* 85 (2014) 352.
4. P. Singh and M.A. Quraishi, *Measurement*, 86 (2016) 114.

5. R. Solmaz. E. Altunbas and G. Kardas, *Mater. Chem. Phys*. 125 (2011) 796.
6. P.C. Okafor, M.E. Ikpi, I.E. Uwaha, E.E. Ebenso, U.J. Ekpe and S.A. Umoren, *Corros. Sci.* 50 (2008) 2310.
7. P.M. Krishnegowda, V.T. Venkatesha, P.K.M. Krishnegowda and S.B. Shivayogiraju, *Ind. Eng. Chem. Res.* 52 (2013) 722.
8. A. Biswas, S. Pal and G. Udayabhanu, *Appl. Surf. Sci*. 353 (2015) 173.
9. N. Soltani, N. Tavakkoli, M.K. Kashani, A. Mosavizadeh, E.E. Oguzie and M.R. Jalali, *J. Ind. Eng. Chem.* 20 (2014) 3217.
10. M. Chevalier, F. Robert, N. Amusant, M. Traisnel, C. Roos and M. Lebrini, *Electrochem. Impedance Spectrosc.* 131 (2014) 96.
11. I.E. Uwah, P.C. Okafor and V.E. Ebiekpe, *Arabian J. Chem*. 6 (2013) 285.
12. F. Suedile, F. Robert, C. Roos and M. Lebrini, *Electrochim. Acta* 133 (2014) 631.
13. S.H. Yoo, Y.W. Kim, K. Chung, S.Y. Baik and J.S. Kim, *Corros. Sci.* 59 (2012) 42.
14. A. Khadraoui, A. Khelifa, M. Hadjmeliani, R. Mehdaoui, K. Hachama, A. Tidu, Z. Azari, I.B. Obot and A. Zarrouk, *J. Mol. Liq.* 216 (2016) 724.
15. M. Farsak, H. Keles and M. Keles, *Corros. Sci.* 98 (2015) 223.
16. G. Das and N. Karak, *Prog. Org. Coat.* 66 (2009) 59.
17. Y. Chen, Y.Y. Jiang, H. Chen, Z. Zhang, J.Q. Zhang and C.N. Cao, *J. Am. Oil. Chem. Soc.* 90 (2013) 1387.
18. N.D. Gowraraju, S. Jagadeesan, K. Ayyasamy, L.O. Olasunkanmi, E.E. Ebenso and C. Subramanian, *J. Mol. Liq.* 232 (2017) 9.
19. Z. Salarvand, M. Amirnasr, M. Talebian, K. Raeissi and S. Meghdadi, *Corros. Sci.* 114 (2017) 133.
20. Y.Y. Jiang, Y. Chen, Z.Y. Ye, H. Chen, Z. Zhang, J.Q. Zhang and C.N. Cao, *Corrosion*, 69 (2011) 672.
21. H.M. Abd El-Lateef, M.A. Abo-Riya and A.H. Tantawy, *Corros. Sci.* 108 (2016) 94.
22. A.J.A. Nasser and M.A. Sathiq, *Arab. J. Chem.* 9 (2016) S691.
23. F. Kurniawan and K.A. Madurani, *Prog. Org. Coat.* 88 (2015) 256.
24. P. Singh, A. Singh and M.A. Quraishi, *J. Taiwan. Inst. Chem. E.* 60 (2016) 588.
25. Y.J. Qiang, S.T. Zhang, L. Guo, S.Y. Xu, L. Feng, I.B. Obot and S.J. Chen, *J. Clean. Prod.* 152 (2017) 17.
26. A.K. Satapathy, G. Gunasekaran, S.C. Sahoo, K. Amit and P.V. Rodrigues, *Corros. Sci.* 51 (2009) 2848.
27. K.G. Zhang, B. Xu, W.Z. Yang, X.S. Yin, Y. Liu and Y.Z. Chen, *Corros. Sci.* 90 (2015) 284.
28. C.B. Verma, M.A. Quraishi and A. Singh, *J. Taiwan. Inst. Chem. Eng.* 49 (2015) 229.
29. M. Bahrami, S. Hosseini and P. Pilvar, *Corros. Sci.* 52 (2010) 2793.
30. Z.Y. Hu, Y.B. Meng, X.M. Ma, H.L. Zhu, J. Li, C. Li and D.L. Cao, *Corros. Sci.* 112 (2016) 563.
31. J. Aljourani, K. Raeissi and M.A. Golozar, *Corros. Sci.* 51 (2009) 1836.
32. N.D. Nam, Q.V. Bui, M. Mathesh, M.Y.J. Tan and M. Forsyth, *Corros. Sci.* 76 (2013) 257.
33. I. Ahamad, R. Prasad and M. Quraishi, *Mater. Chem. Phys.* 124 (2010) 1155.
34. N.D. Nam, Q.V. Bui, M. Mathesh, M.Y.J. Tan and M. Forsyth, *Corros. Sci.* 76 (2013) 257.
35. M.H. Hussin, M.J. Kassim, N.N. Razali, N.H. Dahon and D. Nasshorudin, *Arab. J. Chem.* 9 (2016) S616.
36. G. Gao, C.H. Liang and H. Wang, *Corros. Sci.* 49 (2007) 1833.
37. R. Solmaz, G. Kardas, M. Culha, B. Yazici and M. Erbil, *Electrochim. Acta* 53 (2008) 5941.
38. K. Gu, L. Lv, Z. Lu, H. Yang, F. Mao and J. Tang, *Corros. Sci.* 74 (2013) 408.
39. A.E. Vázquez, G.N. Silva, R.G. Olvera, D.A. Beltrán, H.H. Hernández, M.R. Romo and M.P. Pardavé, *Mater. Chem. Phys.* 145 (2014) 407.
40. M.A. Hegazy, M. Abdallah, M.K. Awad and M. Rezk, *Corros. Sci.* 81 (2014) 54.
41. A. Ghazoui, N. Benchat, F. El-Hajjaji, M. Taleb, Z. Rais, R. Saddik, A. Elaatiaoui and B. Hammouti, *J. Alloy. Compd*. 693 (2017) 510.

42. X.W. Zheng, S.T. Zhang, W.P. Li, L.L. Yin, H. He and J.F. Wu, *Corros. Sci.* 80 (2014) 383.
43. A.K. Singh and M.A. Quraishi, *Corros. Sci.* 53 (2011) 1288.
44. M. Behpour, S.M. Ghoreishi, N. Mohammadi, N. Soltani and M.S. Niasari, *Corros. Sci.* 52 (2010) 4046.
45. A. Popova and M. Christov, *J. Univ. Chemtech. Met.* 43 (2008) 37.
46. M. Abdallah, *Corros. Sci.* 44 (2002) 717.
47. I.A. Ammar and F.M. El Khoraft, *Werkst. Korros.* 24 (1973) 702.
48. R.S. Chaudhary, D.K. Tyagi and A. Kumar, *J. Sci. Ind. Res.* 66 (2007) 835.
49. S. Sanyal and A. Kumar, *J. Indian Chem. Soc.* 87 (2010) 189.
50. S.A. Umoren, E.E. Ebenso and P.C. Okafor, *J. Appl. Polym. Sci.* 103 (2007) 2810.
51. E.E. Oguzie, C. Unaegbu, C.E. Ogukwe, B.N. Okolue and A.I. Onuchukwu, *Mater. Chem. Phys.* 84 (2004) 363.
52. M.A. Quraishi and M.A. Singh, *J. Appl. Electrochem.* 40 (2010) 1293.
53. A.A. Khadom, A.S. Yaro, A. Amir and H. Kadum, *J. Taiwan. Inst. Chem. Eng.* 41 (2010) 122.
54. S. Martinez and I. Sterri, *J. Appl. Electrochem.* 31 (2001) 973.
55. A.Y. Obaid, A.A. Ganash, A.H. Qusti, S.A. Elroby and A.A. Hermas, *Arabian J. Chem*. 10 (2017) S1276.
56. M.V. Fiori-Bimbi, P.E. Alvarez, H. Vaca and C.A. Gervasi, *Corros. Sci.* 92 (2015) 192.